



# AN EXPLORATION OF WATER'S CORE-ATOM AND SURROUNDING CELL SPLITTING: THEORETICAL IMPLICATIONS

#1Mrs.BEERAM JAMUNA, Assistant Professor

#2Mr.AMMASI THIRUGNANAM, Assistant Professor

Department of Physics,

SREE CHAITANYA INSTITUTE OF TECHNOLOGICAL SCIENCES, KARIMNAGAR, TS.

## ABSTRACT:

The NMR investigations of Chen et al. (Magnetic Resonance in Medicine 50, 515-521 2003) revealed that when the magic angle is rotated, the isotropic susceptibility shift divides the water peaks into two distinct peaks. The initial peak in the spectrum can be attributed to the water atoms contained within the core nucleus. Conversely, the second peak can be found in neighboring cells that are in close proximity to the water. This work proposes a theoretical atomic model of the cell based on three-level-type and three-level-cascade atomic configurations. The purpose of this study is to examine the correlation between variation in susceptibility and the distance between water peaks. Additionally, we examine the impact of detunings, the intensity of the electric field and magnetic field, and the angle of magic spinning on the water peak's separation.

**Keywords:** Splitting of water peaks, Magic angle spinning, Nuclear magnetic resonance.

**DOI Number:** 10.48047/nq.2022.20.22.NQ10507

**NeuroQuantology2022;20(22): 4965-4969**

## 1.INTRODUCTION

In many disciplines, such as chemistry, food science, and materials research, nuclear magnetic resonance with high-resolution magic angle spinning (HR-MAS) has become the gold standard for the acquisition of highly resolved spectra and the study of heterogeneous samples with liquid-like dynamics. It may detect phenomena like dipolar interaction, anisotropic chemical shift, and variations in susceptibility at different MAS by keeping the static field direction constant in heterogeneous materials. Figures 2 through Numerous materials, including macromolecular crystals and inorganic solids, have been studied using solid-state nuclear magnetic resonance (NMR). For materials with slower rotation speeds, there are many techniques to obtain resolved spectra. Both live animals and entire organs can be treated using these methods. For instance, side-band suppression by the rotor has been used to perform NMR evaluations of removed human tissues at slower spinning rates. Additionally, the MAT spectra of preserved and living mice's organ and tissue metabolites have been described. Chen et al. reported the proton NMR spectra of

freshly isolated human skeletal muscle samples. Because creatine and phosphocreatine have distinct chemical shifts, the HR-MAS approach can be used to isolate and resolve each compound's <sup>1</sup>H signal. The creatine resonances looked to have two peaks, whereas the phosphocreatine resonance only showed one. Motion-restricted reverberation with increasing linewidth is observed in creatine. Investigating the movement and exchange of water in various animal tissues has attracted a lot of attention in the last several years. Two different peaks appeared under typical liquid conditions as a result of the isotropic susceptibility shift breaking the water resonance in half. The water pool in the dense layer of the outer cell is what causes the greater peak, whereas the free-water cell is what causes the acute peak. Variable angle spinning (VAS) NMR studies were employed by Philp et al. to examine the split water peaks and their impact on the isotope shift mathematical model. This article examines the breaking of water peaks in human cells, which are made up of red blood cells and water. The effects of detunings, magnetic field strength, spinning magic angle, and electric field intensity on water peak splitting in the cell are investigated. We show that the combination of all



three methods increases the water .

**.2. MODEL**

The excitation of light pulses within a medium is investigated, where each medium molecule is made up

of  $\Lambda$ -type

The molecular formula of water and

$\Xi$ -type

In reference to RBCs. Figure 1a shows the energy level configuration of a water atom and Figure 1b shows the same for a red blood cell, both of which assume atom-field interactions. We start by looking at a

possible  $\Lambda$ -type

water atom's atomic system with its three energy levels

$|1\rangle$ ,  $|2\rangle$  and  $|3\rangle$

A weak probe field  $E$  is utilized between layers.

$|1\rangle$  and  $|2\rangle$

with Rabi frequency

$|2\rangle$

In the same way, a strong driving field  $E$  is incorporated between energy eigen state

$|2\rangle$  and  $|3\rangle$

with Rabi frequency

$\Omega_1$

Here,

$\gamma_1$

during the Rabi lunar time

$|1\rangle$  and  $|2\rangle$   $\Gamma_1$

is the decay rate between stages

$|2\rangle$  and  $|3\rangle$

respectively. We consider

three-level cascade

$\Xi$ -type

In turn, respectively. Considered is a three-tiered cascade.

$|a\rangle$ ,  $|b\rangle$  and  $|c\rangle$

Applying the weak probe field  $E$  between

$|a\rangle$  and  $|b\rangle$

$E$  stands for a concentrated laser beam that is intensely focused between

$|b\rangle$  and  $|c\rangle$

The

$\gamma_2$  The rate of degradation that occurs between levels.

$|b\rangle$  and  $|a\rangle$   $\Gamma_2$

is the decay rate between levels

$|c\rangle$  and  $|a\rangle$

respectively.

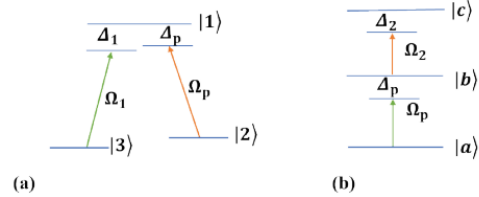


**Figure 1:** [a] Pictures of atomic compounds; [b] Diagrams showing how atoms interact with electromagnetic fields

In order to determine the probing light EP's linear optical susceptibility, we follow the same procedures as in references. Consequently, the following can be said about the interaction image Hamiltonians of these atomic-field systems when the dipole approximation is used:

$$H_w = \frac{-\hbar}{2} (\Omega_p e^{-i\omega_p t} |1\rangle\langle 2| + \Omega_1 e^{-i\omega_1 t} |1\rangle\langle 3|) + H.C \tag{1}$$

$$H_r = \frac{-\hbar}{2} (\Omega_p e^{-i\omega_p t} |b\rangle\langle a| + \Omega_2 e^{-i\omega_2 t} |c\rangle\langle b|) + H.C \tag{2}$$

where the equation (1) The Hamiltonian (2) represents the energy operator for a red blood cell and a water atom. At this location

$\Delta_p$ ,  $\Delta_1$ , and  $\Delta_2$

are the detunings of the probe and driving fields, respectively. Another assumption is that the driving fields are much stronger than the probe field i.e.,

$|\Omega_1|$  and  $|\Omega_k| \gg |\Omega_p|$

and the probe's detunings, respectively, constitute the main field. The probing fields are weak in comparison to the propelling fields, according to an alternative theory.

$$\rho_{12} = (i\Delta_p - \gamma_1)\rho_{12} + i\Omega_p(\rho_{11} - \rho_{22}) + i\Omega_1\rho_{32}, \tag{3}$$

$$\rho_{32} = (i\Delta_p - i\Delta_1 - \Gamma_1)\rho_{32} + i\Omega_1\rho_{12} + i\Omega_p\rho_{31}, \tag{4}$$

$$\rho_{ba} = (i\Delta_p - \gamma_2)\rho_{ba} + i\Omega_p(\rho_{aa} - \rho_{bb}) + i\Omega_2\rho_{ca}, \tag{5}$$

$$\rho_{ca} = (i\Delta_p - i\Delta_2 - \Gamma_2)\rho_{ca} - i\Omega_p\rho_{cb} + i\Omega_2\rho_{ba}, \tag{6}$$

Where

$\gamma_1$ ,  $\gamma_2$ ,  $\Gamma_1$  and  $\Gamma_2$ .

Both Figure 1a and Figure 1b display the system's degradation rates. The water atom is shown in equations (3) and (4), and the red blood cell is shown in equations (5) and (6).

We can calculate the rotor angle and magnetic field, which affect water splitting, according to Chen et al. [5].

$$\Delta v = \left(1 - \sin^2 \frac{\theta}{2}\right) \Delta \chi v.$$



Where

$$v_o = \gamma B_o \text{ and } \Delta\chi = \chi_w - \chi_c.$$

According to Equation(7), the substantial signal splitting

$$\Delta v = \Delta\chi v_o$$

To enhance the visibility of the sample, it might be aligned parallel to the magnetic field. In the case where the lines are perpendicular, we anticipate a modest occurrence of splitting.

$$\Delta v = \frac{\Delta\chi v_o}{2}.$$

To split, a magical angle is required, which is given by

$$\Delta v = \frac{3}{2} \Delta\chi v_o.$$

The computation of the susceptibilities w and c for the water atom and the red blood cell can be achieved by utilizing the models provided.

$$\chi_w = \frac{i\Gamma_1 + i(\Delta_1 - \Delta_p)}{\gamma_1\Gamma_1 + i\gamma_1\Delta_1 - i\gamma_1\Delta_p - i\Gamma_1\Delta_p + \Delta_1\Delta_p - \Delta_p^2 + \Omega_1^2},$$

and,

$$\chi_c = \frac{i\Gamma_2 + i(\Delta_2 - \Delta_p)}{\gamma_2\Gamma_2 + i\gamma_2\Delta_2 - i\gamma_2\Delta_p - i\Gamma_2\Delta_p + \Delta_2\Delta_p - \Delta_p^2 + \Omega_2^2},$$

### 3.RESULTS AND DISCUSSION

By extending the theoretical analysis of water peak splitting, we investigate how variations in electric field, detunings, magnetic field, and rotating angle affect water peak splitting. These factors have the potential to affect the performance of the proposed water-cell system. In the first place, we present a comprehensive elucidation of the phenomenon of water peak splitting by employing an atomic model consisting of two unique cells characterized by disparate susceptibilities. Additionally, we examine the impact of detunings, magnetic field intensity, magic spinning angle, and electric field on the splitting of water peaks. The following is how the corresponding parameters are chosen:

$$\gamma_1 = 1\gamma, \gamma_2 = 1\gamma$$

$$\gamma_3 = 1\gamma, \Delta_1 = 0\gamma, \Gamma_1 = 1.5\gamma, \Gamma_2 = 1.4\gamma, \Delta_2 = -0.5\gamma, \Omega_1 = 2\gamma, \Omega_2 = 1.9\gamma.$$

Figure 2 demonstrates our examination of the impact of different magnetic fields on the division of water peaks. The pink curve in Figure 2 demonstrates that the splitting of water peaks occurs even at low magnetic fields. It is evident that modifying the magnetic field leads to an increase in the height of the split peaks. When the magnetic field strength is 0.8 T, we witness a yellow curve. Similarly, when the magnetic field strength is increased to 0.9 T, we observe a blue curve. Moreover, when the magnetic field reaches a value of B=1 T, the heights of both splitting peaks see a substantial increase, so proving

the profound impact of the magnetic field on the peaks. In this instance, all other parameters remain unchanged, mirroring those of the pink curve. Consequently, the magnitude of the divided peaks can be adjusted to the intended value by altering the magnetic field.

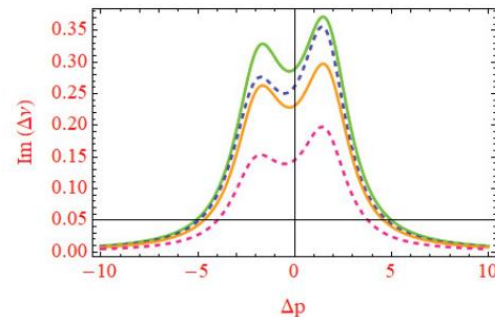


**Figure 2:** Water peak splitting and probe field detunings are compared. We've decided on the following parameters:  $\gamma_1=1\gamma, \gamma_2=1\gamma, \gamma_3=1\gamma, \Gamma_1=1.5\gamma, \Gamma_2=1.4\gamma, \Delta_1=-0.5\gamma, \Omega_1=2\gamma, \Omega_2=1.9\gamma, \theta=\pi/2, B=0.5T, 0.8T, 0.9T$  and  $1T$  (9)

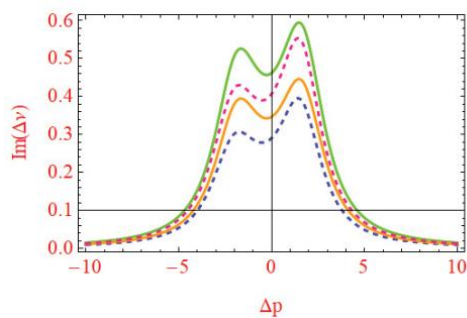
Next, the effect on the dividing water peaks is evaluated by adjusting the rotor's pitch. The connection between the rotor angle  $\theta$  and the division of water peaks is established by Equation (7). Changing the spinning angle affects the spacing of water peaks, as shown in Figure 3. Figure 2 shows that all other parameters are kept constant when the magnetic field strength is set to 1T. As seen by the green curve in Figure 3, the water splitting peaks reach their maximum height at an angle of zero degrees of rotation. With spinning angles kept at 60°, 45°, and 30°, respectively, the pink, yellow, and blue contours in Figure 3 demonstrate that peak height falls with increasing spinning angles. Consequently, the spinning angle is an additional control parameter that can be used to achieve the desired height of water peak separation.

4967

Also, we look at how detunings affect the separation of water peaks. Specifically, we keep all other parameters identical to those in Figure 2 and set the magnetic field intensity to 1 T and the rotation angle to 0°. Water peaks fracturing is observed at different cell detunings, namely,

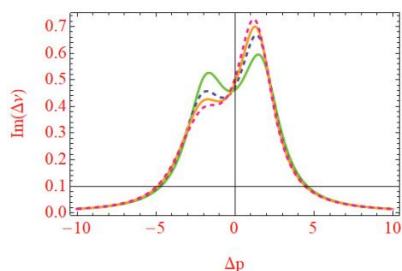
$$\Delta_2 = -0.5\gamma, -1\gamma, -1.5\gamma \text{ and } -2\gamma.$$

Figure 4 shows that when the detunings are changed, the right peak rises and the left peak lowers. The Altering the tunings allows one to modify the vertical extent of the water peak separation, which is another controllable parameter.



**Figure 3:** Detunings in the probe field produce differences in the splitting of water peaks. The settings remain unchanged.

$$\gamma_1=1\gamma, \gamma_2=1\gamma, \gamma_3=1\gamma, \Gamma_1=1.5\gamma, \Gamma_2=1.4\gamma, \Delta_1=-0.5\gamma, \Omega_1=2\gamma, \Omega_2=1.9\gamma, B=IT, \theta=0, \pi/6, \pi/4, \pi/3$$



**Figure 4:** Modifying the detunings and settings of the probe field allows for the separation of water peaks.

$$\gamma_1=1\gamma, \gamma_2=1\gamma, \Gamma_1=1.5\gamma, \Gamma_2=1.4\gamma, \Delta_1=-0.5\gamma, \Omega_1=2\gamma, 2.5\gamma, 3\gamma, 3.2\gamma, \text{ and } \Omega_2=3.5\gamma$$

Furthermore, investigating the effect of the electric field on the separation of water peaks is a worthwhile task. Various electric field intensities and cascading electric fields are selected here.

### Ξ -type

while maintaining all other parameters identical to those shown in Figure 3. In order to investigate the impact of the electric field on the fracturing of water peaks, the susceptibility difference is graphed alongside probe detunings. Furthermore, we have selected a constant electric field within the cascade system, namely,

$$\Omega_2 = 3.5\gamma$$

The green plot in Figure 5 shows how the water peaks are separated.

$$\Omega_1 = 2\gamma$$

When the electric field is consistent, this mechanism produces a noticeable effect.

$$3.2\gamma$$

More particularly, the red curve. The results reveal that raising the field strength allows the water peaks to reach higher heights as compared to the scenario with a weak electric field. According to the graphs, electric power is strongly connected with water divisio

$$\Delta_p = 0\gamma$$

By manipulating the electric field as a stimulating factor,

the height of water peaks can be modified.

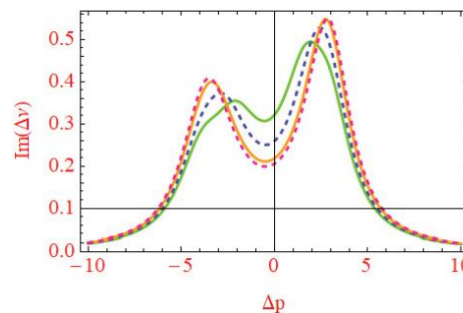


**Figure 5:** To maintain the splitting of water peaks, adjustments are made to the parameters and detunings of the probe field.

$$\gamma_1=1\gamma, \gamma_2=1\gamma, \Gamma_1=1.5\gamma, \Gamma_2=1.4\gamma, \Delta_1=-0.5\gamma, \Omega_1=2\gamma, \Omega_2=1.9\gamma, \Delta_2=0\gamma, -1\gamma, -1.5\gamma, -2\gamma$$

### 4.CONCLUSION

This article provides a detailed explanation of a strategy for changing or manipulating the amplitude of water peaks in an atomic system. A theoretical study was carried out to examine the effects of changing the magnetic field, magic rotating angle, detunings, and electric field on the occurrence of water peak splitting. Each atom in the molecule has atomic configurations that comprise of three levels. This study focused on the discrepancy in vulnerability. Detunings, magnetic fields, externally controlled electric fields, and unknown rotational orientations all have a substantial impact on the splitting of water peaks.

4968

### ACKNOWLEDGEMENT

The Higher Education Commission (HEC) of Pakistan has provided financial support for this initiative under Projects 2421 and 1414.

### REFERENCES

1. Renault, M., et al., Slow-spinning low-sideband HR-MAS NMR spectroscopy: Delicate analysis of biological samples. *Scientific Reports*, **2013**. 3: p. 3349.
2. Mehring, M., High-resolution NMR in solids, 2nd ed., Springer, **1983**.
3. Garroway, A.N., Magic-angle sample spinning of liquids. *J Magn Reson*, **1982**. 49: p. 168-171.
4. Barbara, T.M., Cylindrical demagnetization fields and microprobe design in high-resolution NMR. *J Magn Reson A*, **1994**. 109: p. 265-269.
5. Chen, J.H., et al., Isotropic susceptibility shift under MAS: The origin of the split water resonances in 1H MAS NMR spectra of cell suspensions. *Magn Reson Med*, **2003**. 50(3): p. 515-521.
6. Marti, R.W., et al., High-resolution nuclear magnetic resonance spectroscopy of biological tissues using projected
7. magic angle spinning. *Magn Reson Med*, **2005**.



54(2): p. 253-257.

8. Taylor, J.L., et al., High resolution magic angle spinning proton NMR analysis of human prostate tissue with slow spinning rates. *Magn Reson Med*, **2003**. 50: p. 627-632.
10. Wu, C.L., et al., Proton high-resolution magic angle spinning NMR analysis of fresh and previously frozen tissue

